

## Fine Structure in the Electronic Density of States near the Fermi Energy of Al-Ni-Co Decagonal Quasicrystal from Ultrafast Time-Resolved Optical Reflectivity

T. Mertelj,<sup>1,2</sup> A. Ošlak,<sup>1</sup> J. Dolinšek,<sup>1,2</sup> I. R. Fisher,<sup>3</sup> V. V. Kabanov,<sup>1</sup> and D. Mihailovic<sup>1,2</sup>

<sup>1</sup>*Jozef Stefan Institute, Jamova 39, 1000 Ljubljana, Slovenia*

<sup>2</sup>*Faculty of Mathematics and Physics, University of Ljubljana, Jadranska 21, 1000 Ljubljana, Slovenia*

<sup>3</sup>*Geballe Laboratory for Advanced Materials, Department of Applied Physics, Stanford University, California 94305, USA*

(Received 8 September 2008; published 27 February 2009)

We measured the temperature and fluence dependence of the time-resolved photoinduced optical reflectivity in a decagonal Al<sub>71.9</sub>Ni<sub>11.1</sub>Co<sub>17.0</sub> quasicrystal. We find no evidence for the relaxation of a hot thermalized electron gas as observed in metals. Instead, a quick diffusion of the hot nonthermal carriers  $\sim 40$  nm into the bulk is detected, enhanced by the presence of a broad pseudogap. From the relaxation dynamics we find evidence for the suppression of the electronic density of states (DOS) at the Fermi energy with respect to the electronic DOS at  $\sim 13$  meV away from the Fermi energy which is consistent with recent theoretical calculations.

DOI: 10.1103/PhysRevLett.102.086405

PACS numbers: 71.23.Ft, 71.20.Be, 78.47.jc

The ultrafast relaxation of hot photoexcited electrons in systems with a suppressed density of states (DOS) near the Fermi energy ( $E_F$ ) such as semimetallic graphite [1], cuprates [2], and charge-density wave systems [3] has received a lot of attention in the past two decades. The presence of a gap, or a pseudogap near  $E_F$  leads to a bottleneck in the hot-carrier relaxation and the emission of hot optical phonons [4,5]. The bottleneck can be readily detected by the optical pump-probe spectroscopy.

A suppression of the DOS near  $E_F$  is characteristic also for quasicrystals (QC). [6] The pseudogap is narrow in icosahedral QC ( $i$ -QC) and of the order of  $\sim 1$  eV wide in decagonal QC ( $d$ -QC). It is widely accepted that the narrow pseudogap in  $i$ -QC originates in the Hume-Rothery mechanism [7] which stabilizes the quasiperiodic (QP) order. The role of the Hume-Rothery mechanism and the origin of stability of the quasiperiodic order in  $d$ -QC are much less clear. The electrical conductivity in  $d$ -QC is higher than in  $i$ -QC and clearly metallic along the periodic direction [8] indicating no clear suppression of DOS near  $E_F$ . On the other hand, the electrical conductivity is lower and nonmetallic in the QP plane [8] and there is some theoretical [9] and experimental [10] evidence that a narrow depression of the electronic DOS near  $E_F$  might exist also in  $d$ -QC. It is therefore an interesting fundamental question what are the relaxation pathways of hot photoexcited electrons in  $d$ -QC and whether some information about the structure of DOS near  $E_F$  can be extracted by optical pump-probe spectroscopy which is complementary to more surface sensitive techniques such as photoemission [6] and tunneling [10].

In this Letter we present results of optical pump-probe spectroscopy in a decagonal Al<sub>71.9</sub>Ni<sub>11.1</sub>Co<sub>17.0</sub> QC. From the relaxation dynamics we find evidence for a decrease in the electronic DOS at  $E_F$  with respect to DOS on a scale of  $\sim 13$  meV away from  $E_F$  energy and no evidence for the relaxation of a hot *thermalized* electron gas [11]. This

indicates that the electronic DOS around  $E_F$  in Al-Ni-Co  $d$ -QC is not energy independent like in a simple metal in accord with recent theoretical calculation [9].

The preparation and characterization of a single grain decagonal Al<sub>71.9</sub>Ni<sub>11.1</sub>Co<sub>17.0</sub> quasicrystal was described elsewhere [12]. Optical measurements were performed on a side facet, which is parallel to the tenfold axis of the prism shaped sample mounted in an optical cryostat. A standard pump-probe setup was used with linearly polarized pump beam with the photon energy 1.55 eV, the pulse length 50 fs and repetition frequency 250 kHz. The pump beam was focused to a 250- $\mu$ m diameter spot on the facet in a nearly perpendicular geometry. To detect the photoinduced reflectivity  $\Delta R/R$  a weaker probe beam with the photon energy,  $\hbar\omega_{\text{probe}}$ , either 1.55 or 3.1 eV and the diameter 220  $\mu$ m was focused to the same spot and detected upon reflection by a  $p$ - $i$ - $n$  photodiode.

In Fig. 1(a) we show the dependence of the  $\Delta R/R$  transients on the probe polarization at two different photon energies at the temperature 5 K. We can identify three distinct time scales on which the transients show different behavior. On the sub-ps time scale one can clearly identify a sub-ps component with fast  $\sim 200$ -fs rise and decay times. The component is present in all traces except for the polarization along QP direction at 3.1 eV probe-photon energy (PPE) where another component is revealed, which slowly rises on a few-ps time scale after initial  $\sim 100$ -fs rise. At an intermediate time scale between  $\sim 1$  and  $\sim 20$  ps we observe further rise of the  $\Delta R/R$  which only starts to relax towards equilibrium after  $\sim 2$  ps with 3.1-eV PPE and after  $\sim 10$  ps with 1.55-eV PPE. The dispersion of the  $\Delta R/R$  rise indicates a two component relaxation on this time scale as well. On a long time scale beyond  $\sim 20$  ps all curves, when properly scaled, fall onto each other indicating a common origin of the relaxation.

To study further the temperature and pump fluence ( $\mathcal{F}$ ) dependence we chose 1.55-eV PPE and the polarization

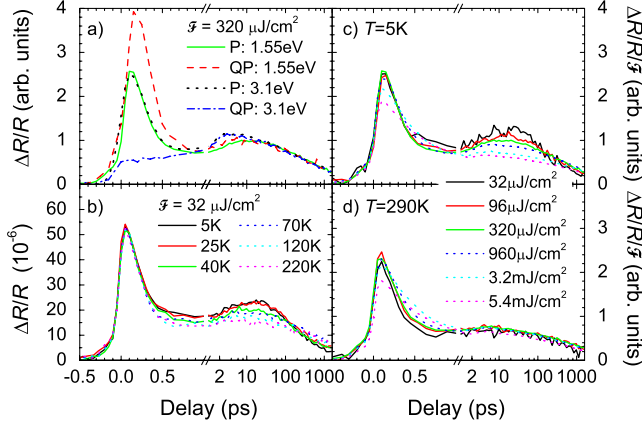


FIG. 1 (color online). The probe polarization and photon energy dependence of photoinduced-reflectivity transients at 5 K (a). The scans are normalized to enable easier comparison. Temperature dependence of photoinduced-reflectivity transients (b) and fluence dependence of photoinduced-reflectivity transients at two different temperatures (c) and (d) at 1.55-eV probe-photon energy and polarization along the periodic direction.

along the periodic direction which has the largest signal-to-noise ratio and contains all relaxation components [13]. In Fig. 1(b) we show the temperature dependence of the transients at the lowest  $\mathcal{F}$ . The sub-ps component is clearly temperature independent, while at the intermediate time scale a shift of the  $\Delta R/R$  peak towards shorter delay and decrease of the peak amplitude are observed with an increasing temperature.

The  $\mathcal{F}$  dependence at 5 K [Fig. 1(c)] is somewhat similar to the temperature dependence, except that at the highest two  $\mathcal{F}$  the sub-ps component shows saturation and an increase of the relaxation time. At 290 K [Fig. 1(d)] the increase of the  $\mathcal{F}$  only influences the sub-ps component, while the relaxation beyond  $\sim 1$  ps is  $\mathcal{F}$  independent.

We start the analysis by considering the long time scale first. The universal delay dependence at different polarizations and PPE indicates that on this time scale all the subsystems are in a local thermal equilibrium and can be described by a single local temperature. Because of the experimental geometry the time dependence of the local temperature is governed by the 1D heat diffusion equation. Since the optical penetration depth at the probe-photon energies, as determined from the angular dependence of the reflectivity, is  $\sim 25$  nm, we assume that  $\Delta R/R$  is in the lowest order proportional to the surface temperature rise  $\Delta T_s(t)$ .

If, after a local temperature is established, the energy is distributed within the surface layer of depth  $z_0$ , the time dependence of the surface temperature is obtained from the solution of the 1D heat diffusion equation,

$$\Delta T_s(t) = \frac{\Delta T_0}{\sqrt{1 + \frac{4Dt}{z_0^2}}}, \quad (1)$$

where  $D$  represents the heat diffusivity along the QP direction in our experimental geometry [14]. Equation (1) fits the measured  $\Delta R/R$  on the long time scale rather well [see Figs. 2(a) and 2(b)] except for low  $\mathcal{F}$  at low  $T$ , where the temperature dependence of  $D$  and nonlinear dependence of  $\Delta R/R$  on  $\Delta T_s$  become important. From the fits we determine the energy deposition depth  $z_0$  and the initial temperature rise  $\Delta T_0$  using published values of the heat capacity [15,16] and thermal conductivity along the QP direction [15,17].  $z_0$ , shown in Fig. 2(c), first increases and then drops slowly with increasing  $T$  to  $\sim 40$  nm at 290 K. Although we obtain at 5 K virtually the same  $z_0$  from measurements at two different  $\mathcal{F}$  the values below  $\sim 100$  K should be taken with caution due to the limited validity of Eq. (1).

Surprisingly, at all temperatures  $z_0$  is significantly larger than the optical penetration depth of  $\sim 25$  nm indicating a quick diffusion of hot carriers into the sample during the first few picoseconds of relaxation. This is rather unexpected due to the strong Drude damping in the QP plane [17]. One can roughly estimate the hot electron diffusion constant by neglecting the energy transfer to the lattice,  $D_{el} = \lambda_{el}/c_{el}\rho$ , where  $\lambda_{el}$  is the electronic heat conductivity,  $c_{el}$  the electronic heat capacity, and  $\rho$  the mass density. We calculate  $\lambda_{el}$  from resistivity [12], which is almost  $T$  independent, using the Wiedemann-Franz law. By taking  $c_{el}$  from [17] we obtain  $D_{el} \approx 1$  cm<sup>2</sup>/s, which is virtually temperature independent. In 1 ps this gives 20 nm diffusion length which is of correct magnitude to explain observations.

We proceed with the analysis of the intermediate time scale. Temperature dependencies of the peak amplitude and the intermediate-time scale rise time shown in Fig. 3 clearly suggest that there exists a well-defined energy scale

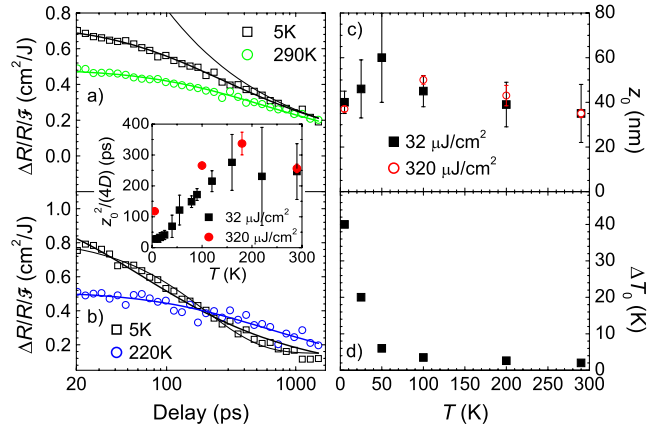


FIG. 2 (color online). Fits of Eq. (1) to  $\Delta R/R$  at  $\mathcal{F} = 320 \mu\text{J}/\text{cm}^2$  (a) and at  $\mathcal{F} = 32 \mu\text{J}/\text{cm}^2$  (b) shown by the thick solid lines. For comparison a function proportional to  $1/\sqrt{t}$  in (a) and a single exponential fit in (b) are shown by the thin solid lines. The inset shows the temperature dependence of the fit parameter. The temperature dependence of the initial energy-deposition depth (c) and the initial surface-temperature rise at  $32\text{-}\mu\text{J}/\text{cm}^2$  excitation fluence (d).

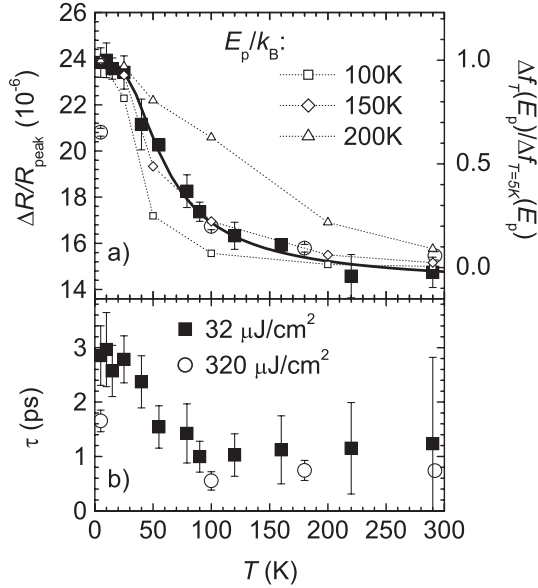


FIG. 3. Temperature dependencies of the intermediate-time scale peak magnitude of  $\Delta R/R$  (a) and the intermediate-time scale rise time (b) at the two different fluences. In (a) the small open symbols connected with dotted lines represent  $\Delta f_T(E_p)$  discussed in text. The solid line is a fit of Eq. (3) to the data.

of the order of  $\sim 100$  K associated with the processes occurring on this time scale. We assume that  $\Delta R$  is a consequence of the excited state absorption [18],

$$\Delta R \propto \int d\epsilon N(\epsilon) |M(\epsilon, \omega)|^2 [f(\epsilon) - f_T(\epsilon)], \quad (2)$$

where  $\hbar\omega$  is the energy of the photons,  $\epsilon$  the energy measured from the Fermi energy,  $N(\epsilon)$  is the effective density of the initial states close to the Fermi energy [19],  $M(\epsilon, \omega)$  the effective dipole transition matrix element,  $f(\epsilon)$  the nonequilibrium electron distribution function, and  $f_T(\epsilon)$  the equilibrium Fermi function. If  $N(\epsilon)$  has in addition to a smooth background a narrow peak at the energy  $E_p$  there will exist a contribution  $\Delta R_p$  to  $\Delta R$  proportional to  $f(E_p) - f_T(E_p)$  in addition to a weakly temperature dependent contribution  $\Delta R_b$  from the smooth background.

In the simplest case one can assume that the nonequilibrium distribution is thermal,  $f(E_p) = f_{T'}(E_p)$ , at an elevated temperature which is the same as the lattice temperature  $T' = T + \Delta T_0$ , where  $\Delta T_0$  is estimated from the long time scale behavior. In Fig. 3(a) we show the difference  $\Delta f_T(E_p) = f_{T'}(E_p) - f_T(E_p)$  for three different  $E_p$  using values of  $\Delta T_0$  from Fig. 2(d). It is clearly seen that  $\Delta f_T(E_p)$  at  $E_p/k_B = 150$  K reproduces the measured temperature dependence rather well if one assumes that  $\Delta R_b$  is temperature independent.

The alternative scenario is the existence of a bottleneck due to the suppressed density of states near the Fermi energy similar to the pseudogap in the cuprate superconductors. In this case for small excitation densities and

strong bottleneck the density of the photoexcited quasiparticles is given by [4],

$$n_{pe} \propto 1/[1 + B \exp(-\Delta_g/k_B T)], \quad (3)$$

where  $\Delta_g$  represents the pseudogap width and  $B$  the ratio between the number of phonon degrees of freedom and the number of electronic states in the phonon-energy range. A fit of Eq. (3) to the data is shown in Fig. 3(a). As in the previous case we assumed that  $\Delta R$  is a sum of a temperature independent part  $\Delta R_b$  and a part proportional to Eq. (3). The resulting pseudogap width is virtually the same as in the previous case,  $\Delta_g/k_B = 140 \text{ K} \pm 40 \text{ K}$ . The large error bar comes from indeterminacy of  $\Delta R_b$ .

Both models are based on an increased density of states at  $\sim 13$  meV away from the Fermi energy and are just two limiting cases representing either no or a strong bottleneck. In the strong bottleneck case  $\Delta R_{peak}/R$  is proportional to  $\mathcal{F}$  at small  $\mathcal{F}$  while at large  $\mathcal{F}$  a crossover to  $\Delta R_{peak}/R \propto \sqrt{\mathcal{F}}$  is expected [4]. We do not observe any of the dependencies in our case. On the other hand, the  $\mathcal{F}$  dependence of  $\Delta R_{peak}/R$  for small  $\mathcal{F}$  in the no-bottleneck model is compatible with the experimental one shown in Fig. 4. Unfortunately, the no-bottleneck model fails to fit the data beyond  $\mathcal{F} \approx 1 \text{ mJ/cm}^2$  as well. The reason for this might be in  $\mathcal{F}$  dependence of  $\Delta R_b$ , which also shows some saturation beyond  $\mathcal{F} \approx 3 \text{ mJ/cm}^2$  judging from the measurements at 290 K [see Fig. 1(d)].

While the  $\mathcal{F}$  dependence clearly excludes the strong bottleneck scenario it does not exclude a weak bottleneck, the presence of which is suggested by the increase of the intermediate-scale rise time below 100 K [see Fig. 3(b)]. In order to elaborate this we need to analyze the response on the shortest time scale first.

The sub-ps peak amplitude has linear  $\mathcal{F}$  dependence and the decay time has no  $\mathcal{F}$  dependence up to  $\mathcal{F} \approx 3 \text{ mJ/cm}^2$ . In addition, both show no  $T$  dependence so the sub-ps dynamics cannot be attributed to the thermal

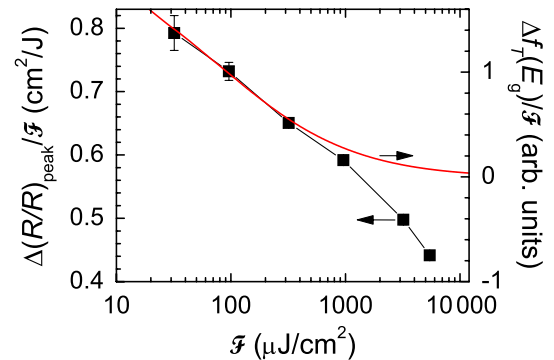


FIG. 4 (color online). Fluence dependence of the intermediate-time scale peak magnitude of  $\Delta R/R$  at 5 K. For comparison  $\Delta f_T(E_p)$  is shown with  $E_p/k_B = 150$  K as the solid line assuming 45-nm initial energy deposition depth and published values of the heat capacity data [15–17] in similar decagonal quasicrystals.



relaxation [11] where  $f(\epsilon)$  is assumed to be the Fermi distribution with the nonequilibrium electronic temperature  $T_e$ .  $f(\epsilon)$  is therefore nonthermal on the sub-ps time scale and the sub-ps peak is due to the relaxation across the broad pseudogap [6,20] and the hot carriers diffusion into the sample. The broad pseudogap suppresses the probability for the creation of the low energy electron-hole ( $e$ - $h$ ) pairs increasing the electron thermalization time beyond  $\sim 500$  fs enhancing the hot-carrier diffusion into the sample. There is also no evidence for the thermal relaxation of the hot electron gas on the longer a-few-picosecond time scale. The intermediate-time scale rise time increases with decreasing temperature, which is inconsistent with the thermal relaxation [11], where the relaxation time is predicted to be proportional to the lattice temperature  $T_L$  for  $T_e \sim T_L$ .

The intermediate-time scale dynamics might therefore at least in part be attributed to the dynamic lattice expansion due to an increasing lattice temperature [21]. The expansion, however, also cannot explain the increase of the intermediate-time scale rise time at low temperatures, implying another relatively slow relaxation channel. We tentatively assign this channel to the relaxation of hot nonthermal optical phonons. We believe that due to the increased thermalization time a significant number of hot optical phonons is generated in addition to the low energy  $e$ - $h$  pairs during the thermalization. These nonthermal hot optical phonons can decay by the anharmonic decay or by excitation of the  $e$ - $h$  pairs. At low temperatures the anharmonic decay channel is suppressed resulting in a bottleneck and the increase of the intermediate-time scale rise time below 100 K.

A rather narrow  $\sim 300$ -meV pseudogap of the electronic DOS in Al-Ni-Co  $d$ -QC was recently predicted theoretically [9]. In our experiment the energy scale of  $\sim 13$  meV does not correspond to the width of the pseudogap but rather to the distance of the Fermi energy from the closest edge of the gap. This is consistent with the calculations [9] where the Fermi energy is shifted towards the high energy edge of the gap. Such a shift is qualitatively consistent with the photoemission data [6] where only the pseudogap states below the Fermi energy could be reliably observed. In addition, the absence of any finer structure of DOS in the photoemission might also originate from the extreme sensitivity of the photoemission to the surface DOS which is predicted [9] to show no narrow pseudogap contrary to the bulk DOS in Al-Ni-Co  $d$ -QC.

In conclusion, the relaxation upon photoexcitation in Al<sub>71.9</sub>Ni<sub>11.1</sub>Co<sub>17.0</sub> quasicrystal therefore proceeds roughly in two steps. In the first step the presence of the broad pseudogap slows down the hot-carrier thermalization. During the relatively slow thermalization hot carriers diffuse up to  $\sim 40$  nm into the bulk and a part of the absorbed energy goes to the nonthermal hot optical phonons. During the second step, which is at 5 K characterized by the relaxation time of  $\sim 3$  ps, the hot nonthermal phonons

decay. At low temperatures the nonthermal-phonon decay is suppressed due to the decrease of the anharmonic relaxation rate and the weak bottleneck in the relaxation through the electronic channel. The bottleneck is a consequence of a relative decrease of the electronic DOS at the Fermi energy with respect to the electronic DOS at  $\sim 13$  meV from the Fermi energy, which is consistent with recent theoretical predictions [9].

- 
- [1] K. Seibert, G. C. Cho, W. Kütt, H. Kurz, D. H. Reitze, J. I. Dadap, H. Ahn, M. C. Downer, and A. M. Malvezzi, Phys. Rev. B **42**, 2842 (1990).
  - [2] S. G. Han, Z. V. Vardeny, K. S. Wong, O. G. Symko, and G. Koren, Phys. Rev. Lett. **65**, 2708 (1990).
  - [3] J. Demsar, K. Biljaković, and D. Mihailovic, Phys. Rev. Lett. **83**, 800 (1999).
  - [4] V. Kabanov, J. Demsar, B. Podobnik, and D. Mihailovic, Phys. Rev. B **59**, 1497 (1999).
  - [5] T. Kampfrath, L. Perfetti, F. Schapper, C. Frischkorn, and M. Wolf, Phys. Rev. Lett. **95**, 187403 (2005).
  - [6] Z. M. Stadnik, D. Purdie, M. Garnier, Y. Baer, A.-P. Tsai, A. Inoue, K. Edagawa, S. Takeuchi, and K. H. J. Buschow, Phys. Rev. B **55**, 10938 (1997).
  - [7] E. Belin-Ferre, J. Phys. Condens. Matter **14**, R789 (2002).
  - [8] S. Martin, A. F. Hebard, A. R. Kortan, and F. A. Thiel, Phys. Rev. Lett. **67**, 719 (1991).
  - [9] M. Krajčí, J. Hafner, and M. Mihalkovič, Phys. Rev. B **73**, 134203 (2006).
  - [10] J. Okada, T. Ekino, Y. Yokoyama, T. Takasaki, Y. Watanabe, and S. Nanao, J. Phys. Soc. Jpn. **76**, 033707 (2007).
  - [11] P. B. Allen, Phys. Rev. Lett. **59**, 1460 (1987).
  - [12] I. R. Fisher, M. Kramer, Z. Islam, A. Ross, A. Kracher, T. Wiener, M. Sailer, A. Goldman, and P. Canfield, Philos. Mag. B **79**, 425 (1999).
  - [13] We found that the  $T$  and  $\mathcal{F}$  dependence at 3.1-eV PPE is similar to behavior at 1.55-eV PPE.
  - [14] For simplicity we assume that the initial temperature is given by  $\Delta T_0(z) = \Delta T_0 \exp(-z^2/z_0^2)$  and that  $D$  is  $T$  independent.
  - [15] J. A. Barrow, B. A. Cook, P. C. Canfield, and D. J. Sordelet, Phys. Rev. B **68**, 104202 (2003).
  - [16] A. Inaba, R. Lortz, C. Meingast, J. Q. Guo, and A. P. Tsai, J. Alloys Compd. **342**, 302 (2002).
  - [17] A. D. Bianchi, F. Bommeli, E. Felder, M. Kenzelmann, M. A. Chernikov, L. Degiorgi, H. R. Ott, and K. Edagawa, Phys. Rev. B **58**, 3046 (1998).
  - [18] D. Dvorsek, V. V. Kabanov, J. Demsar, S. M. Kazakov, J. Karpinski, and D. Mihailovic, Phys. Rev. B **66**, 020510 (2002).
  - [19] We assume that on the time scale of a few ps the final states, which are  $\hbar\omega$  away from the Fermi energy are completely unoccupied and that the optical resonance is broad with respect to  $k_B T$ .
  - [20] M. Krajčí, J. Hafner, and M. Mihalkovič, Phys. Rev. B **62**, 243 (2000).
  - [21] C. Richardson and J. Spicer, Appl. Phys. Lett. **80**, 2895 (2002).